

Blue Fluorescent Dihydro-indenoindene Derivatives with Unusual Low Oxidation Potentials for Multifunctional OLEDs Materials

Yi Wei,^{*,†} Wei-Jyun Wang,[†] Yu-Ting Huang,[†] Bo-Cheng Wang,[†] Wen-Hao Chen,[†] Sang-Hsiu Wu,[†] Chiu-Hui He[‡]

[†]No.151, Yingzhuan Rd., New Taipei City 25137, Taiwan (R.O.C.)

[‡]No. 88, Sec. 4, Tingchow Rd., Taipei City, 11677, Taiwan (R.O.C.)

Email: ywei@mail.tku.edu.tw

SUPPLEMENTARY INFORMATION

(23 pages)

Table of Content

General information -----	S2
Experimental procedures and characterization for 1–3 -----	S3-S5
Absorption and Emission Spectra for 3a–c -----	S6
CV voltammograms for 3a–c -----	S6
Device details for 3a–c and NPB -----	S7
¹ H and ¹³ C NMR spectra for 1–3 -----	S10-S19
DFT Calculation data for 3a–c -----	S20-S23
References-----	S23

General information

All reactions regarding air or moisture sensitive compounds were performed in dry reaction vessels under nitrogen or argon atmosphere. Analytical thin-layer chromatography (TLC) was performed on Merck 60 F₂₅₄ silica gel plates, indicated by UVP UVGC-25 Compact UV Lamp. Visualization was accomplished with UV light. Fractional flash column chromatography was carried out using 32-63 µm silica gel.

Materials All reagents were purchased from Acros Organic, Sigma-Aldrich, TCI, or Alfa-Aesar, used directly without further purification. Solvents used for experiments were reagent grade unless mentioned elsewhere. Diethyl ether and toluene were advanced dried over Na with benzophenone-ketyl intermediate as an indicator.

Instruments ¹H NMR and ¹³C NMR spectra were recorded on a Bruker AVANCE III HD (600 MHz ¹H, 150 MHz ¹³C) spectrometer in CD₂Cl₂ with tetramethylsilane or CH₂Cl₂ as an internal reference. Chemical shifts (δ) and coupling constants (J) are reported in ppm and Hz, respectively. Splitting patterns are described as following: doublet, d; triplet, t; quartet, q; multiplet, m. Data are reported as δ (splitting pattern, J). Mass and High-resolution mass spectra were recorded on LCQ Advantage GC/LC/MS and Finnigan MAT 95S spectrometers. Data are reported in m/z. Combustion analyses were performed on a PerkinElmer 2400-CHN analyzer by the Northern Instrument Center of Taiwan. Absorption spectra were measured on a Thermo Scientific Evolution 60S spectrophotometer using spectrophotometric CH₂Cl₂. Upon excitation, emission spectra were measured on a JASCO FP-6500 fluorescence spectrometer in the same solutions. Fluorescence quantum yields were measured using Coumarin 1 (99% in EtOAc)¹ as a standard. Cyclic voltammetry (CV) experiments were performed in dichloromethane solutions containing 0.1 M tetrabutylammonium perchlorate as a supporting electrolyte on a CHI 611D Electrochemical analyzer. Platinum, carbon, and Ag/AgCl electrodes were used as counter, working, and reference electrodes respectively. Differential scanning calorimetry (DSC) analyses were performed on a METTLER TOLEDO DSC 1 differential scanning calorimeter. Sample was heated (10 °C/min) to melt and then cooled rapidly by liquid nitrogen. Melting point was obtained during the heating progress. T_g was recorded during the second round of heating (10 °C/min). Thermogravimetric analyses (TGA) were performed on a PerkinElmer Pyris 1 TGA thermogravimetric analyzer.

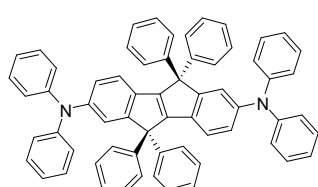
5,5,10,10-Tetraphenyl-5,10-dihydroindeno[2,1-a]indene (**1**)

To a 250 mL, three-necked, round-bottomed flask was placed a solution of (*Z*)-2,2'-dibromostilbene² (6761 mg, 20 mmol) in diethyl ether (100 mL). The reaction flask was cooled to 0 °C, and *n*-BuLi (1.6 M in hexanes, 27.5 mL, 44 mmol) was added dropwise. It was stirred at this temperature for 30 minutes followed by adding a solution of benzophenone (8018 mg, 44 mmol) in diethyl ether (20 mL). The resulting mixture was gradually warmed to ambient temperature and then quenched with saturated NaHCO₃ (*aq*) (50 mL). After filtration, the precipitants were washed by distilled water (100 mL) and hexanes (100 mL), and then dried under reduced pressure. The crude residue dissolved in acetic acid (50 mL) was placed in another 100 mL, two-necked, round-bottomed flask. HCl (12 N, 36 μL, 1 mmol) was then added and the reaction mixture was refluxed for 2 hours. After cooling to ambient temperature, saturated NaHCO₃ (*aq*) (50 mL) was added again and stirred vigorously for 20 minutes. The precipitation was filtered and the yellow solids were washed by distilled water (100 mL), methanol (100 mL), and hexanes (100 mL) in turn, and then dried under reduced pressure to give **1**, which was further re-crystallized from CH₂Cl₂ to afford 2441 mg of pure **1** (24 %): *T_m* 376 °C (DSC); M.W.: 508.65; ¹H NMR (600 MHz, CDCl₃) δ 7.42 (dd, *J* = 6.8, 1.8, 2H), 7.30-7.23 (m, 20H), 7.18-7.11 (m, 6H); ¹³C NMR (150 MHz, CD₂Cl₂) δ 157.7, 155.7, 143.0, 138.6, 128.7, 128.6, 127.4, 127.3, 126.2, 125.3, 121.1, 63.4; EI-MS (negative) calcd for C₄₀H₂₈ [M[−]]: 508.2, found: 508.3; TLC R_f 0.75 (CH₂Cl₂/hexanes, 1/3).

2,7-Dibromo-5,5,10,10-tetraphenyl-5,10-dihydroindeno[2,1-a]indene (**2**)³

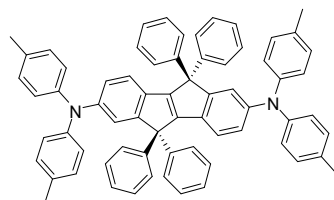
To a 250 mL, three-necked, round-bottomed flask was placed a suspension of **1** (1017 mg, 2 mmol), CuBr₂ (3350 mg, 15 mmol), and Al₂O₃ (10050 mg) in CCl₄ (20 mL). The reaction mixture was heated to reflux for 16 hours. After cooling to ambient temperature, the excess amount of CuBr₂ and Al₂O₃ were filtered thru Celite. The filtrate was evaporated under reduced pressure and re-crystallized from toluene to afford 1093 mg of pure **2** (82 %): *T_m* 393 °C (DSC); M.W.: 666.44; ¹H NMR (600 MHz, CD₂Cl₂) δ 7.54 (d, *J* = 1.7, 2H), 7.31-7.24 (m, 22H), 7.03 (d, *J* = 8.2, 2H); ¹³C NMR (150 MHz, CD₂Cl₂) δ 159.6, 155.2, 141.8, 137.3, 130.7, 129.0, 128.7, 128.5, 127.7, 122.3, 120.4, 63.6; TLC R_f 0.70 (CH₂Cl₂/hexanes, 1/3); Anal. Calcd for C₄₀H₂₆Br₂: C, 72.09, H, 3.93. Found: C, 72.30, H, 3.94.

2,7-Bis(*N,N*-diphenylamino)-5,5,10,10-octaphenyl-5,10-dihydroindeno[2,1-a]indene (**3a**)⁴



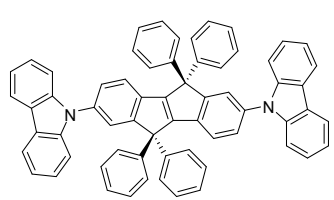
To a 25 mL, two-necked, round-bottomed flask was placed **2** (666 mg, 1 mmol), Pd₂(dba)₃ (18 mg, 0.02 mmol), NaO(*t*-Bu) (288 mg, 3 mmol), P(*t*-Bu)₃ (0.03 M in toluene, 2 mL, 0.06 mmol), and diphenylamine (372 mg, 2.2 mmol) in toluene (20 mL). The reaction mixture was refluxed for 4 hours. After cooling to ambient temperature, it was filtered and the precipitant was washed by toluene (100 mL). The crude residue was sublimated at 383 °C under 5 × 10⁻⁶ Torr to afford 573 mg of pure **3a** (68 %): *T_m* 363 °C (DSC); *T_d* 492 °C (TGA); *T_g* 163 °C (DSC); M.W.: 843.06; ¹H NMR (600 MHz, CD₂Cl₂) δ 7.23 (s, 20H), 7.20 (d, *J* = 2.0, 2H), 7.16 (t, *J* = 15.8, 8H), 6.99–6.94 (m, 24H), 6.74 (dd, *J* = 8.2, 2.0, 2H); ¹³C NMR (150 MHz, CD₂Cl₂) δ 158.7, 154.1, 147.9, 146.1, 143.3, 133.4, 129.4, 128.7, 128.6, 127.1, 124.4, 123.1, 122.5, 121.4, 120.9, 63.3; TLC *R_f* 0.75 (CH₂Cl₂/hexanes, 1/3); HR-ESI-MS (positive) calcd for C₆₄H₄₆N₂ [M⁺]: 842.3661, found: 842.3693; Anal. Calcd for C₆₄H₄₆N₂: C, 91.18, H, 5.50, N, 3.32. Found: C, 90.99, H, 5.42, N, 3.59.

2,7-Bis(*N,N*-di-(*p*-tolyl)-amino)-5,5,10,10-octaphenyl-5,10-dihydroindeno[2,1-a]indene (**3b**)



To a 25 mL, two-necked, round-bottomed flask was placed **2** (666 mg, 1 mmol), Pd₂(dba)₃ (18 mg, 0.02 mmol), NaO(*t*-Bu) (288 mg, 3 mmol), P(*t*-Bu)₃ (0.03 M in toluene, 2 mL, 0.06 mmol), and di-*p*-tolylamine (434 mg, 2.2 mmol) in toluene (20 mL). The reaction mixture was refluxed for 4 hours. After cooling to ambient temperature, it was filtered and the precipitant was washed by toluene (100 mL). The crude residue was sublimated at 393 °C under 5 × 10⁻⁶ Torr to afford 557 mg of pure **3b** (62 %): *T_m* 433 °C (DSC); *T_d* 514 °C (TGA); *T_g* 165 °C (DSC); M.W.: 899.17; ¹H NMR (600 MHz, CD₂Cl₂) δ 7.23 (s, 20H), 7.15 (d, *J* = 2.0, 2H), 6.98 (d, *J* = 8.3, 8H), 6.91 (d, *J* = 8.3, 2H), 6.86 (d, *J* = 8.3, 8H), 6.65 (dd, *J* = 8.3, 2.0, 2H), 2.25 (s, 12H); ¹³C NMR (150 MHz, CD₂Cl₂) δ 158.6, 153.8, 146.5, 145.6, 143.6, 132.9, 130.0, 128.8, 128.6, 127.1, 124.7, 121.4, 120.7, 120.4, 63.3, 20.8; TLC *R_f* 0.75 (CH₂Cl₂/hexanes, 1/3); HR-ESI-MS (positive) calcd for C₆₈H₅₄N₂ [M⁺]: 898.4287, found: 898.4313; Anal. Calcd for C₆₈H₅₄N₂: C, 90.83, H, 6.05, N, 3.12. Found: C, 90.72, H, 5.98, N, 3.30.

Bis(9-carbazolyl)-5,5,10,10-octaphenyl-5,10-dihydroindeno[2,1-a]indene (**3c**)



To a 25 mL, two-necked, round-bottomed flask was placed **2** (666 mg, 1 mmol), Pd₂(dba)₃ (18 mg, 0.02 mmol), NaO(*t*-Bu) (288 mg, 3 mmol), P(*t*-Bu)₃ (0.03 M in toluene, 2 mL, 0.06 mmol), and carbazole (368 mg, 2.2 mmol) in toluene (20 mL). The reaction mixture was refluxed for 4 hours. After cooling to ambient temperature, it was filtered and the precipitant was washed by toluene (100 mL). The crude residue was sublimated at 393 °C under 5 × 10⁻⁶ Torr to afford 537 mg of pure **3c** (64 %): *T_m* 435 °C (DSC); *T_d* 546 °C (TGA); *T_g* 204 °C (DSC); M.W.: 839.03; ¹H NMR (600 MHz, CD₂Cl₂) δ 8.10 (d, *J* = 7.8, 4H), 7.71 (s, 2H), 7.46–7.44 (m, 12H), 7.36–7.30 (m, 20H), 7.23–7.23 (m, 4H); ¹³C NMR (150 MHz, CD₂Cl₂) δ 159.5, 142.6, 141.0, 137.5, 136.0, 129.1, 128.7, 128.7, 127.7, 126.2, 126.0, 124.2, 123.7, 122.1, 120.5,

120.3, 110.1, 63.8; TLC R_f 0.75 (CH₂Cl₂/hexanes, 1/3); HR-ESI-MS (positive) calcd for C₆₄H₄₂N₂Na [M²⁺+Na]: 442.1572, found: 442.2563; Anal. Calcd for C₆₄H₄₂N₂: C, 91.62, H, 5.05, N, 3.34. Found: C, 91.46, H, 4.98, N, 3.56.

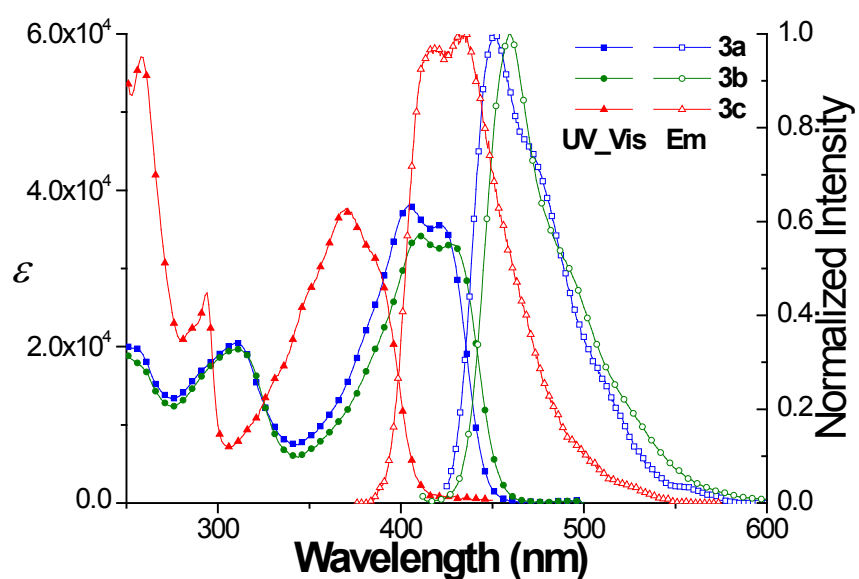


Figure S1. Stacked Plots of the Absorption and Emission Spectra for **3a–c**.

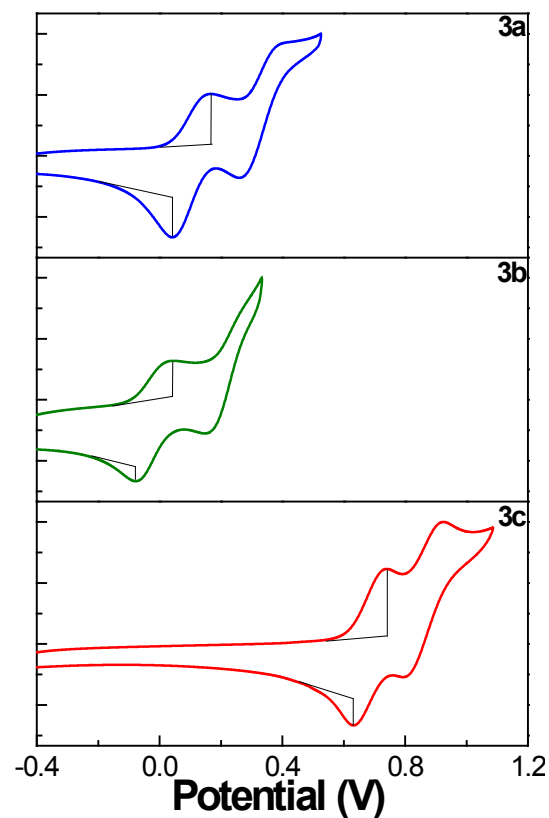


Figure S2. Plots of the Cyclic Voltammograms for **3a–c**.

Device fabrication and measurements

All the materials were commercially available or synthesized as described, and subjected to gradient sublimation twice prior to use. The cathode was an indium tin oxide (ITO) coated glass with the sheer resistance of $\sim 30 \Omega/\square$. Pre-patterned ITO substrate was cleaned sequentially by sonication in detergent solution, doubly distilled water, and EtOH for 5 min in turn before blow-drying with a stream of nitrogen. Advanced surface cleaning was accomplished by oxygen plasma treatment for 3 min. hole injection layer (HIL) was then spin-coated at a rate of 3000 rpm on the substrate before it was loaded into the vacuum chamber. Furthermore, a layer by layer deposition was carried out thermally at a rate of 0.1-0.3 nm/s under a pressure of 5×10^{-6} Torr. Electroluminescence efficiencies and spectra were recorded on a Keithley 2400 source meter and Photo Research PR-655 SpectraScan spectroradiometer, respectively. All the measurements were made at atmospheric conditions. Device configurations are described as following: Hole-only device, ITO/NPB (40 nm)/**3a** (50 nm)/NPB (40 nm)/Anode; electron-only device, ITO/BCP (40 nm)/**3a** (50 nm)/TPBI (40 nm)/LiF (1 nm)/Anode; A, ITO/electron transporting layer (ETL)/EL/ETL/electron injection layer (EIL)/Anode; A, ITO/emitting layer (EL)/electron transporting layer (ETL)/electron injection layer (EIL)/Anode; B, ITO/HTL/EL/ETL/EIL/Anode; C and E, ITO/HTL/EL/EIL/Anode; D, ITO/HIL/EL/ETL/EIL/Anode, where HIL, HTL, EM, ETL, EIL, and Anode correspond to 30 nm of PEDOT:PSS, 20 nm of **3a** or 40 nm of NPB, 40 nm of **3a-c** or **Alq₃**, 40 nm of TPBI, 1 nm of LiF, and 150 nm of Al, respectively.

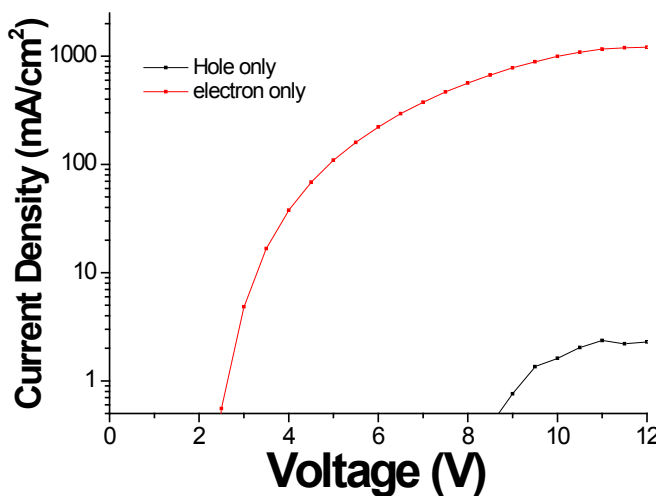


Figure S3. Stacked Plots of the I - V Curves in Hole and Electron Only Devices for **3a**.

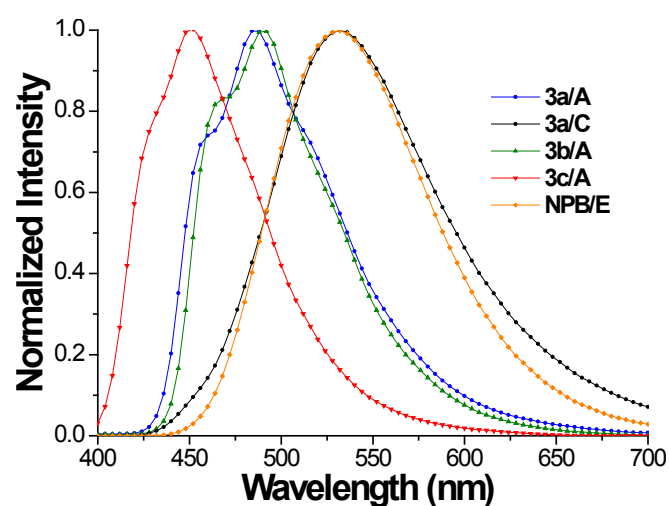


Figure S4. Stacked Plots of the EL Spectra for **3a–c** and NPB.

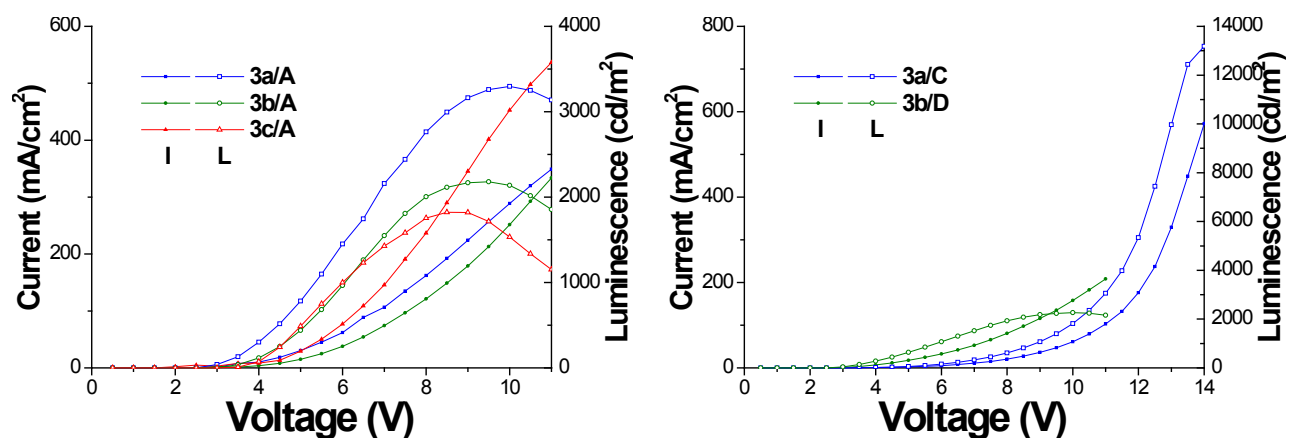


Figure S5. Stacked Plots of the *I*–*V*–*L* Curves for **3a–c**.

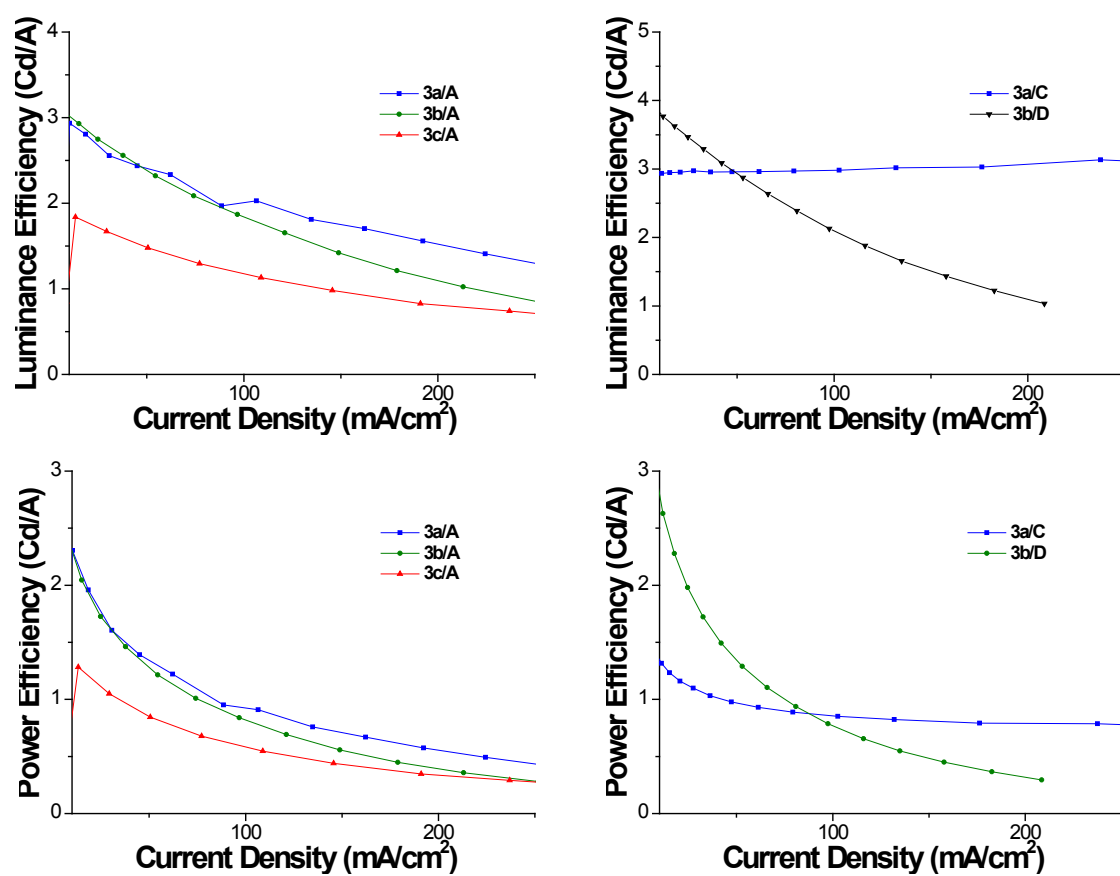
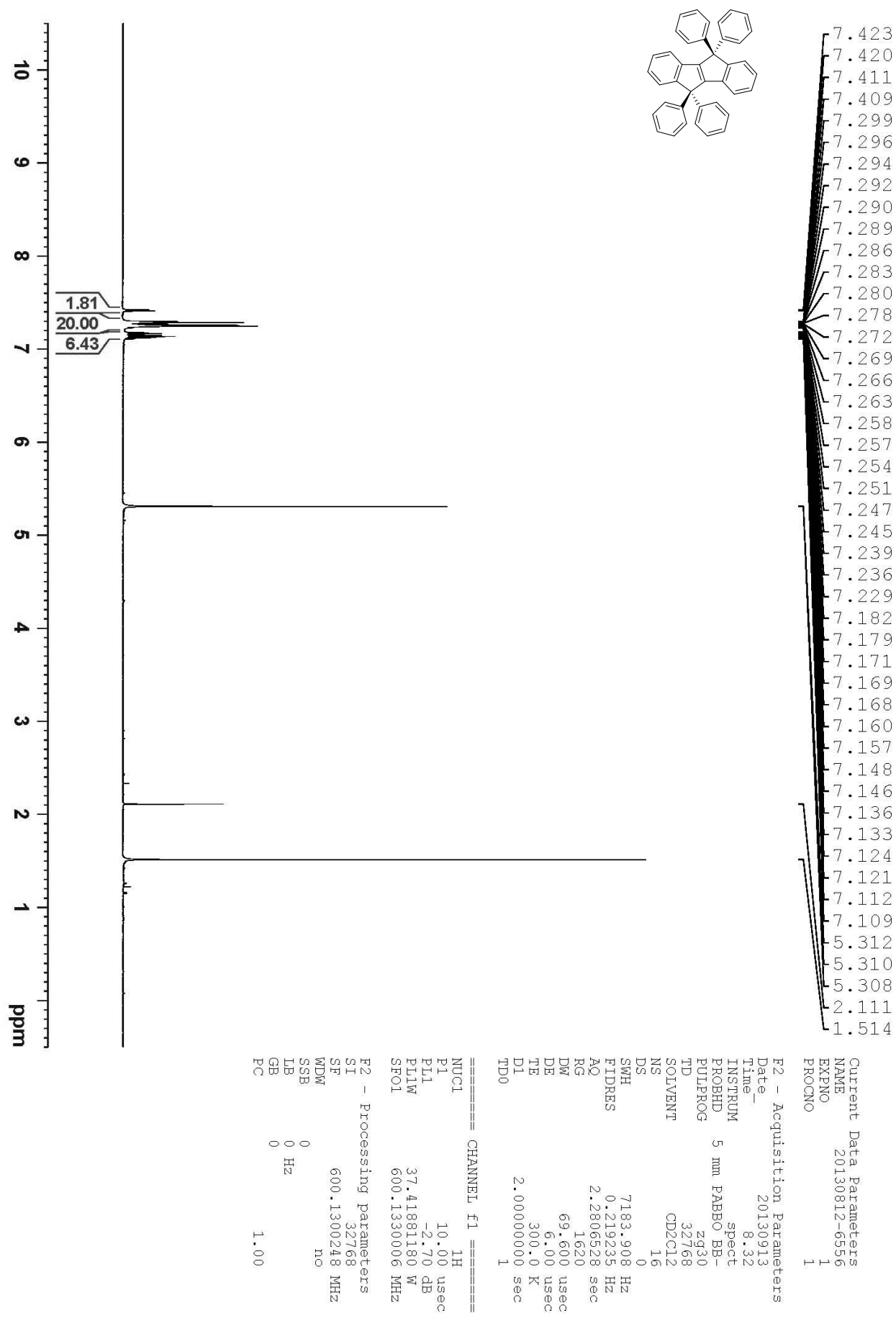
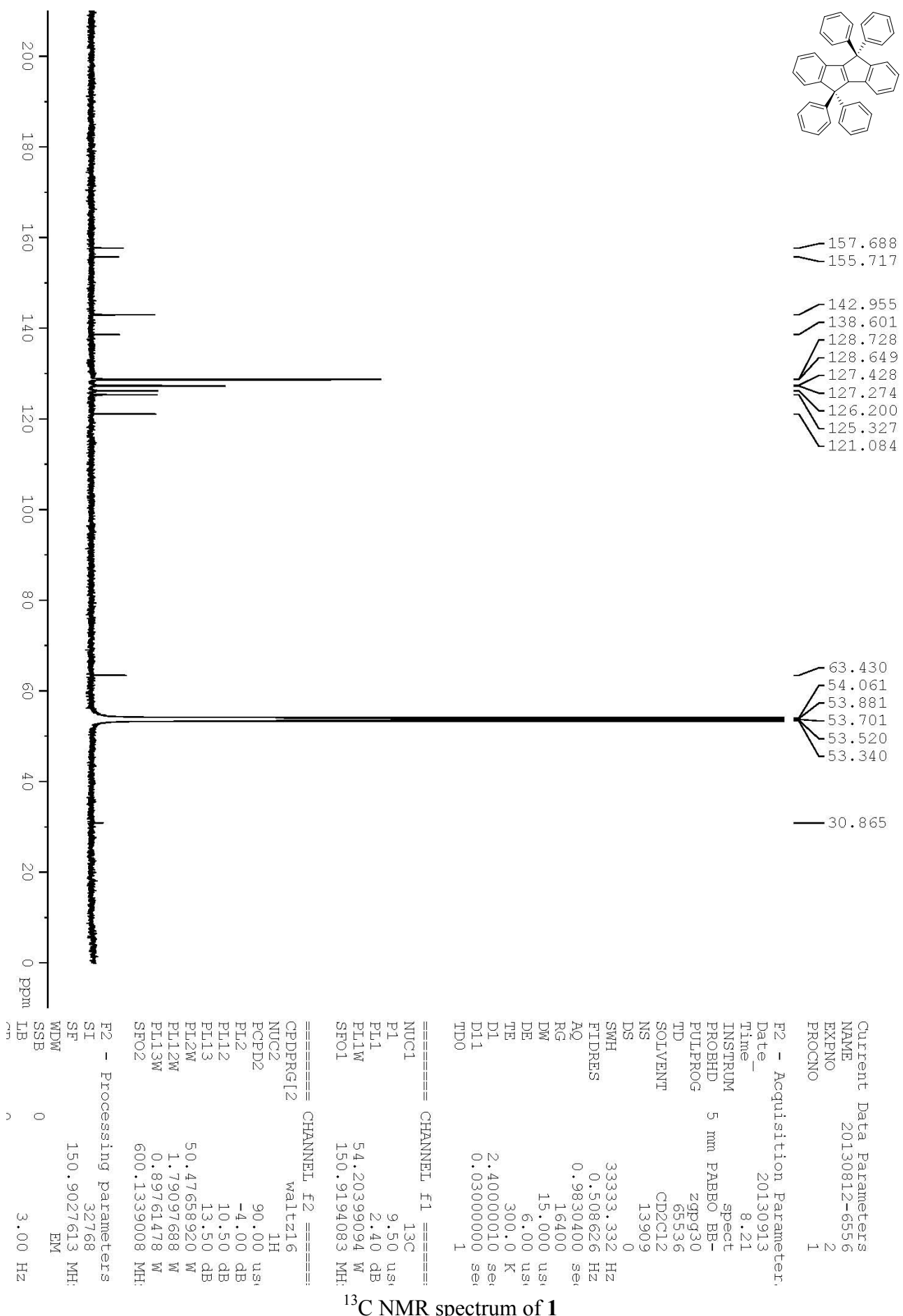
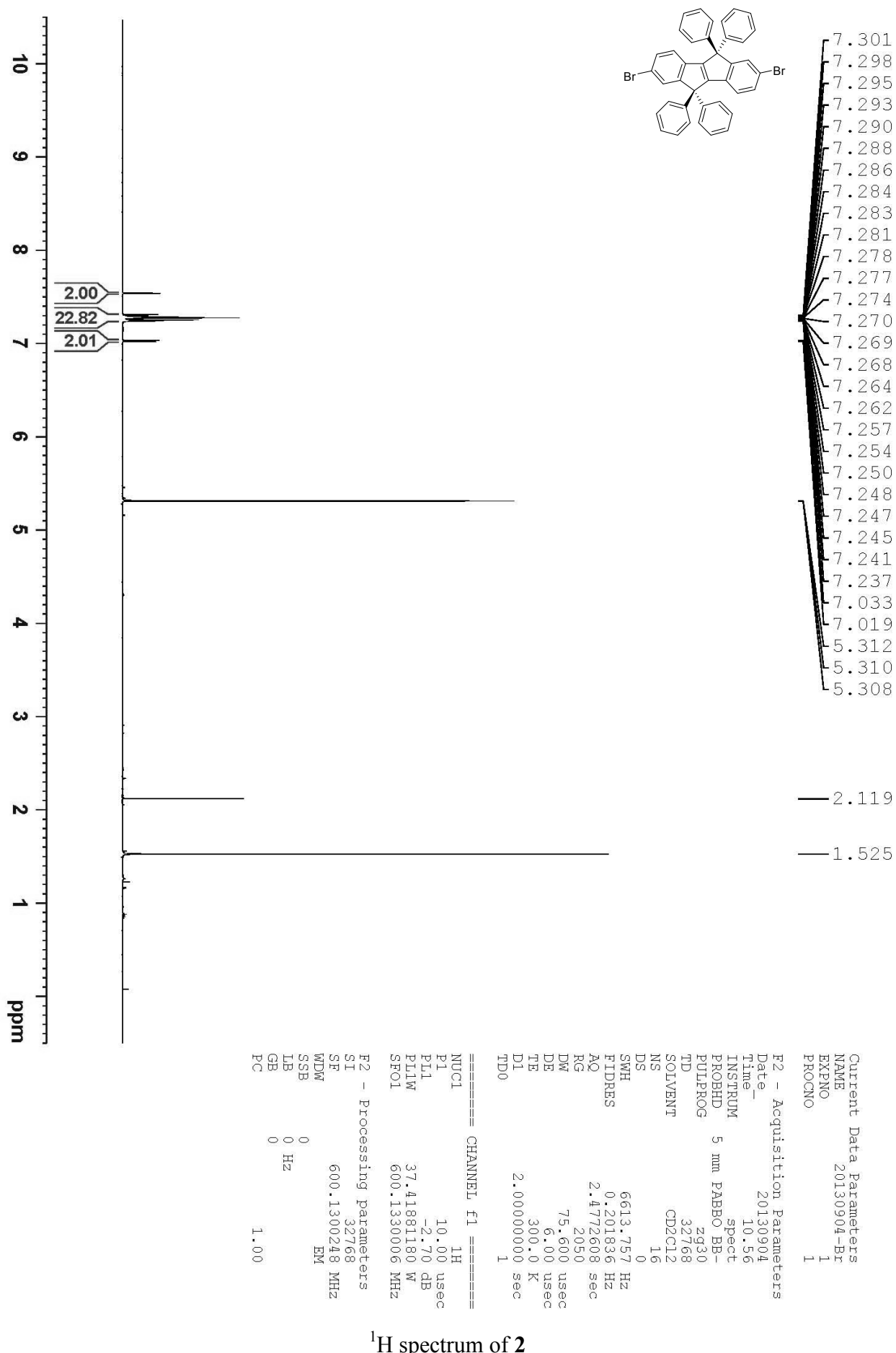


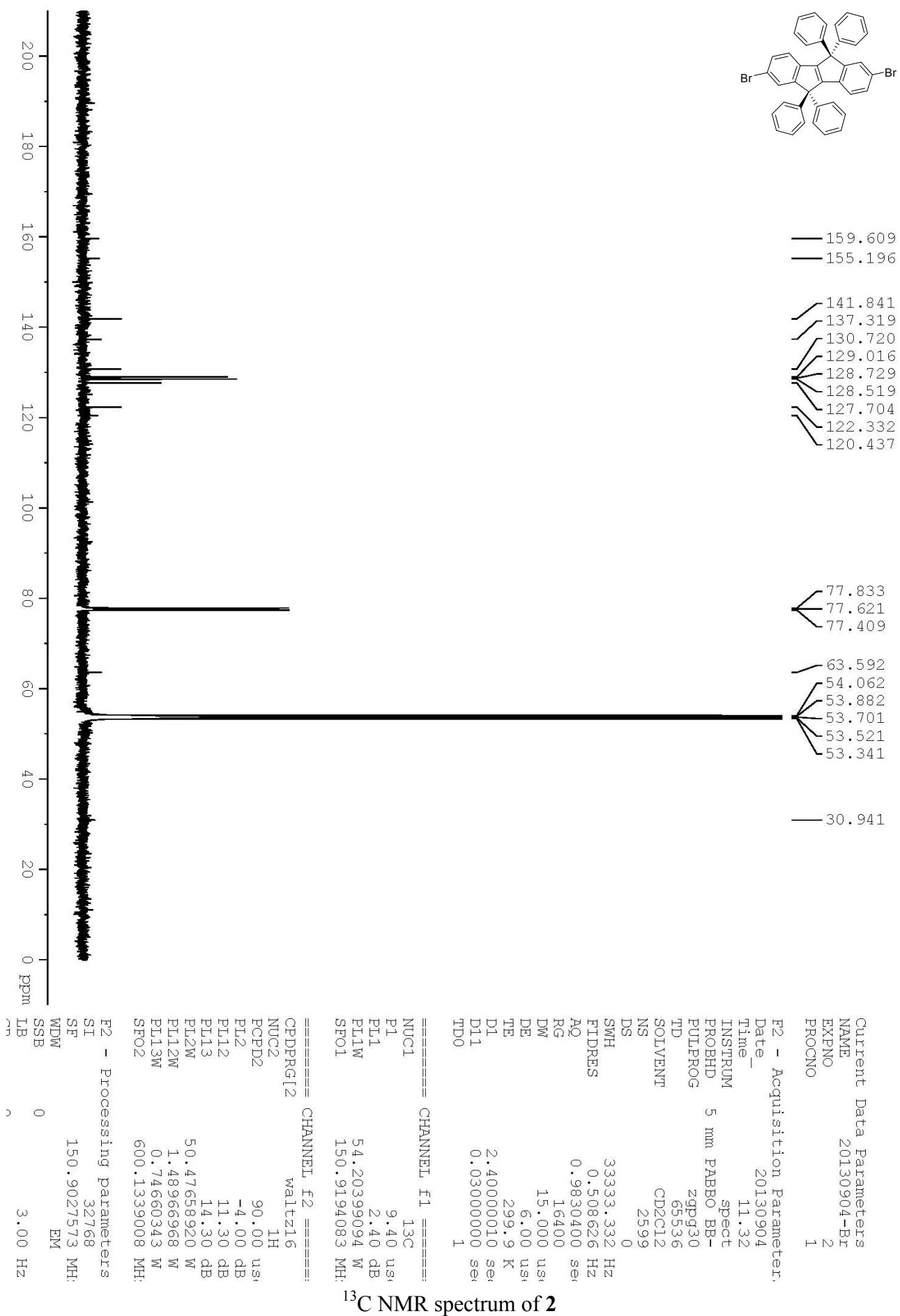
Figure S6. Stacked Plots of the $I-\eta_c$ and $I-\eta_p$ Curves for **3a–c**.

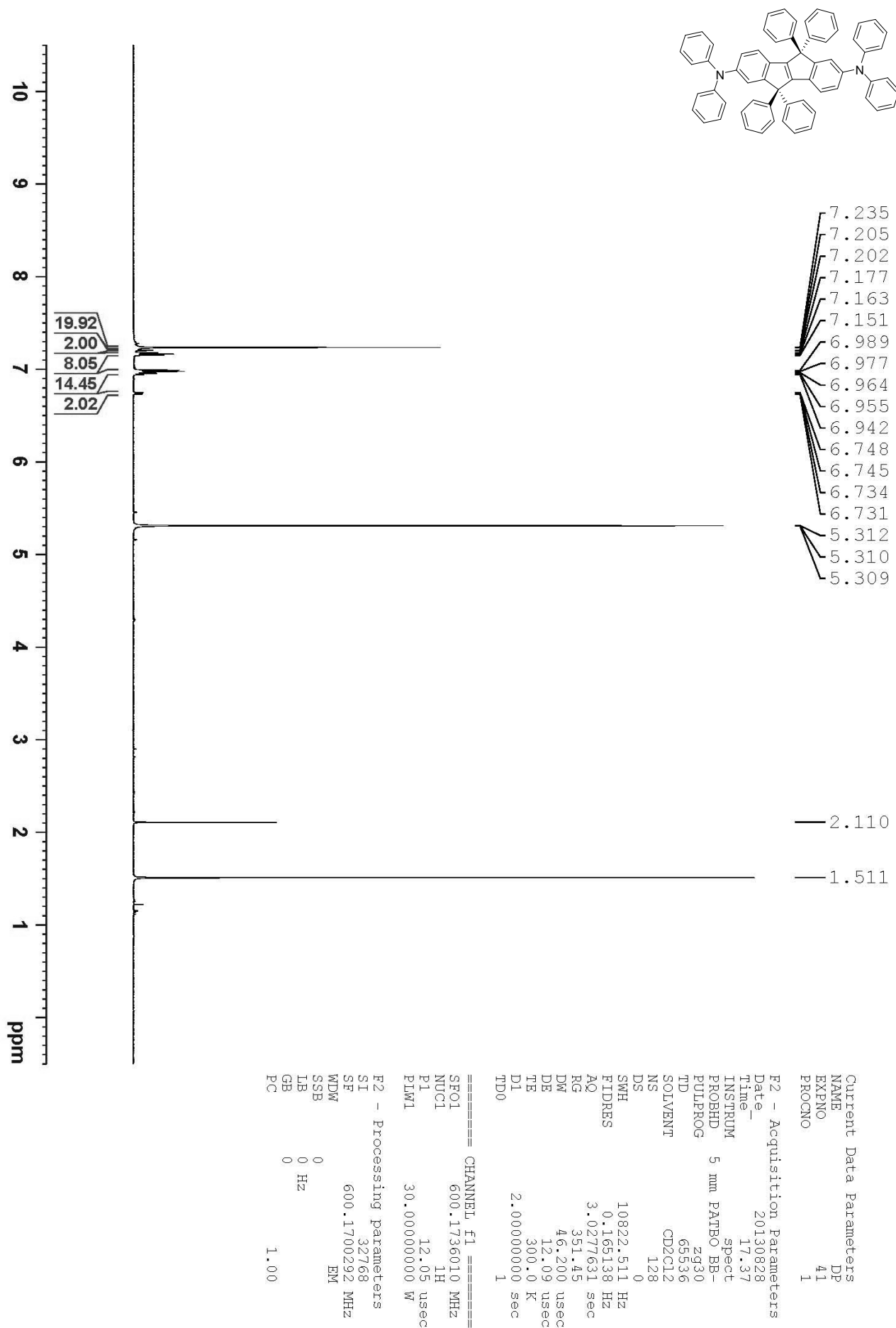


¹H spectrum of **1**

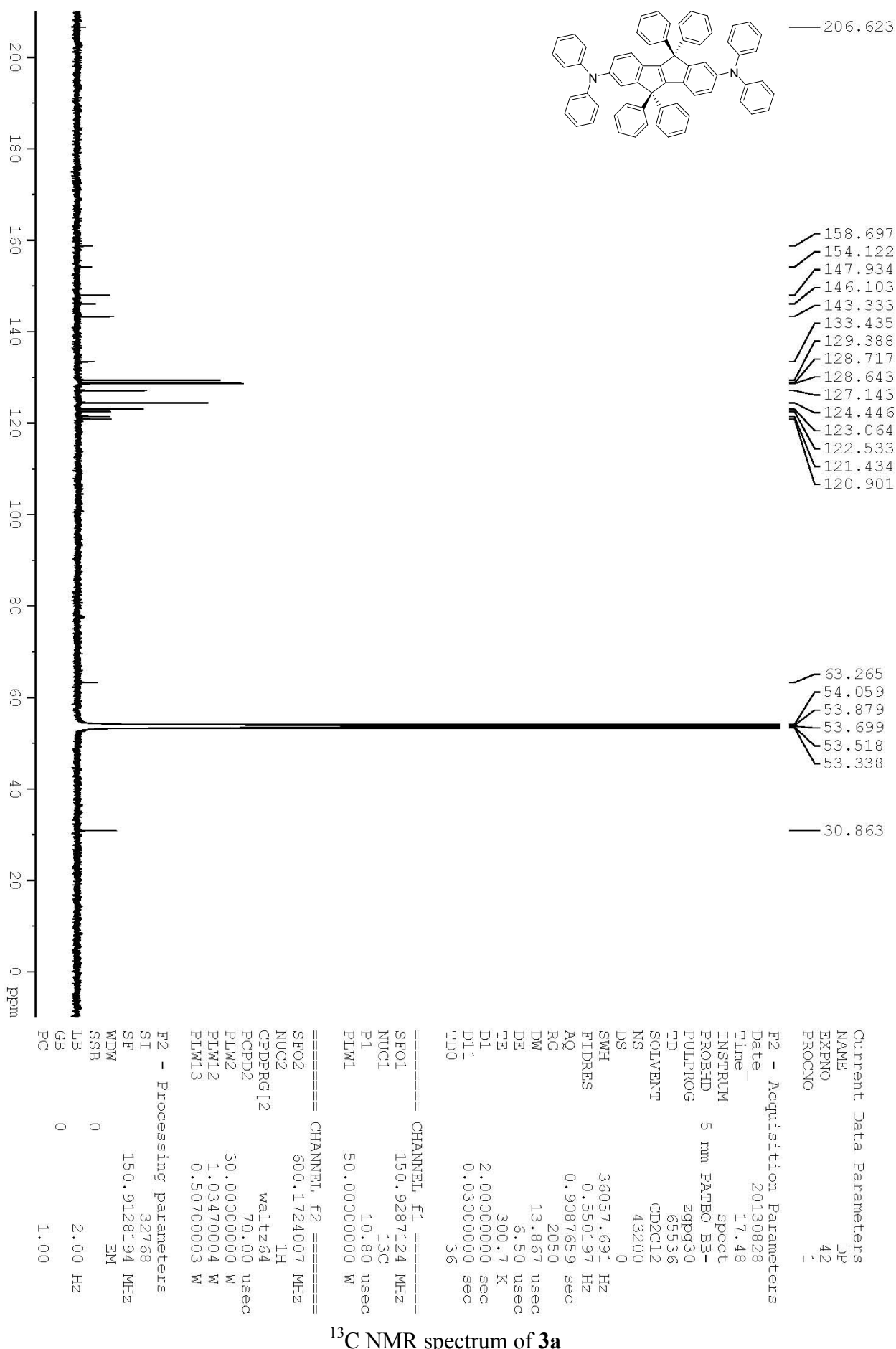


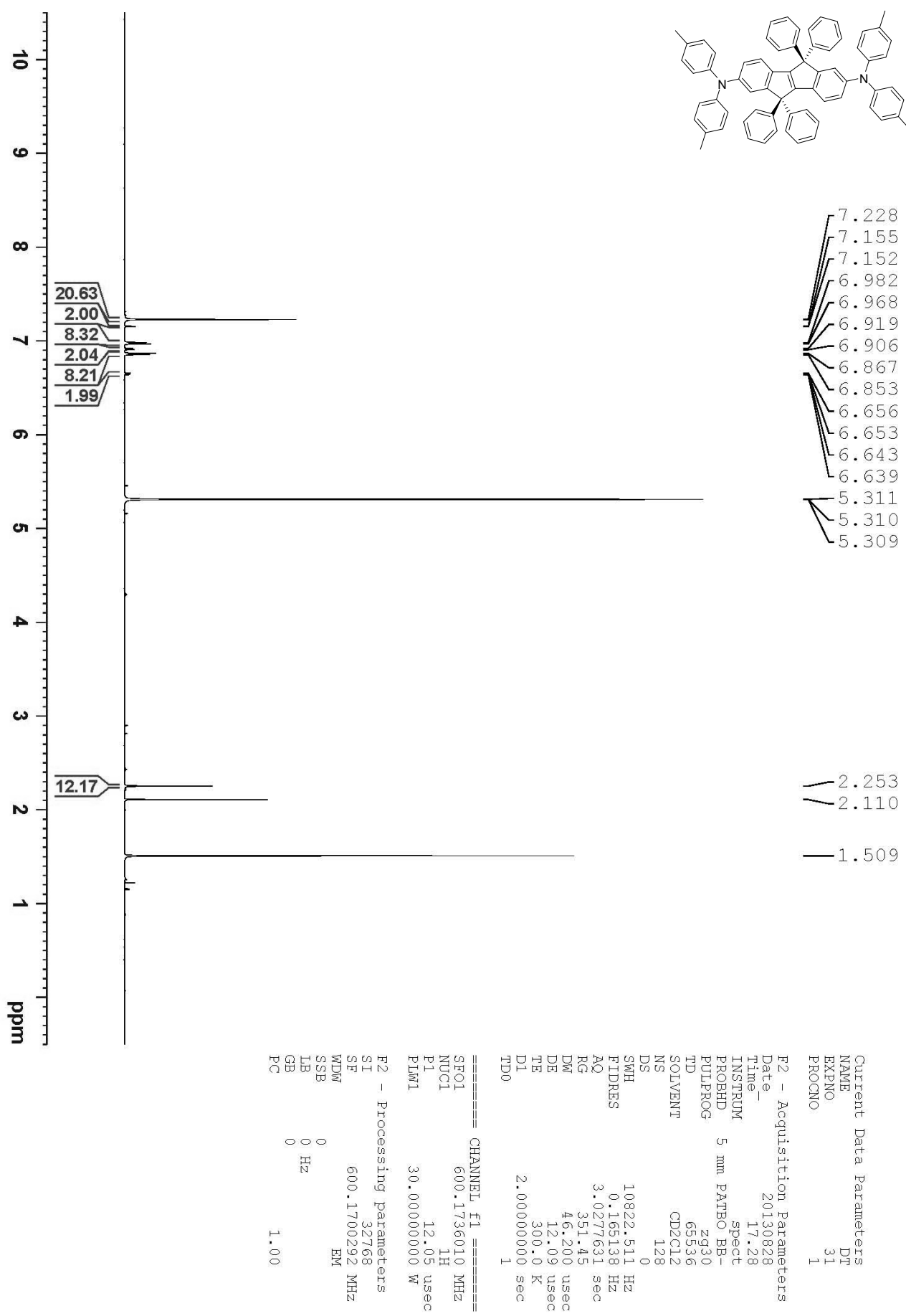




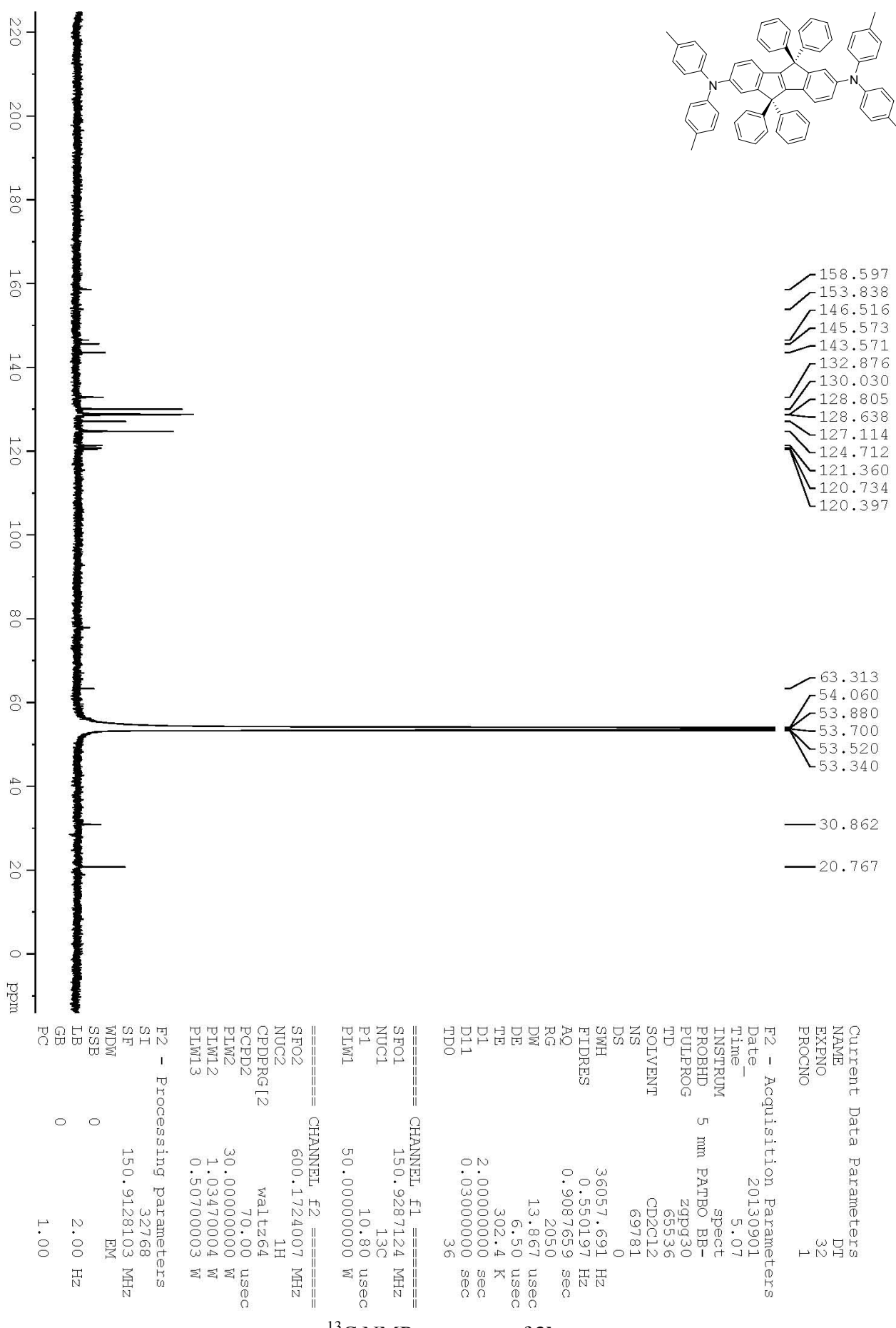


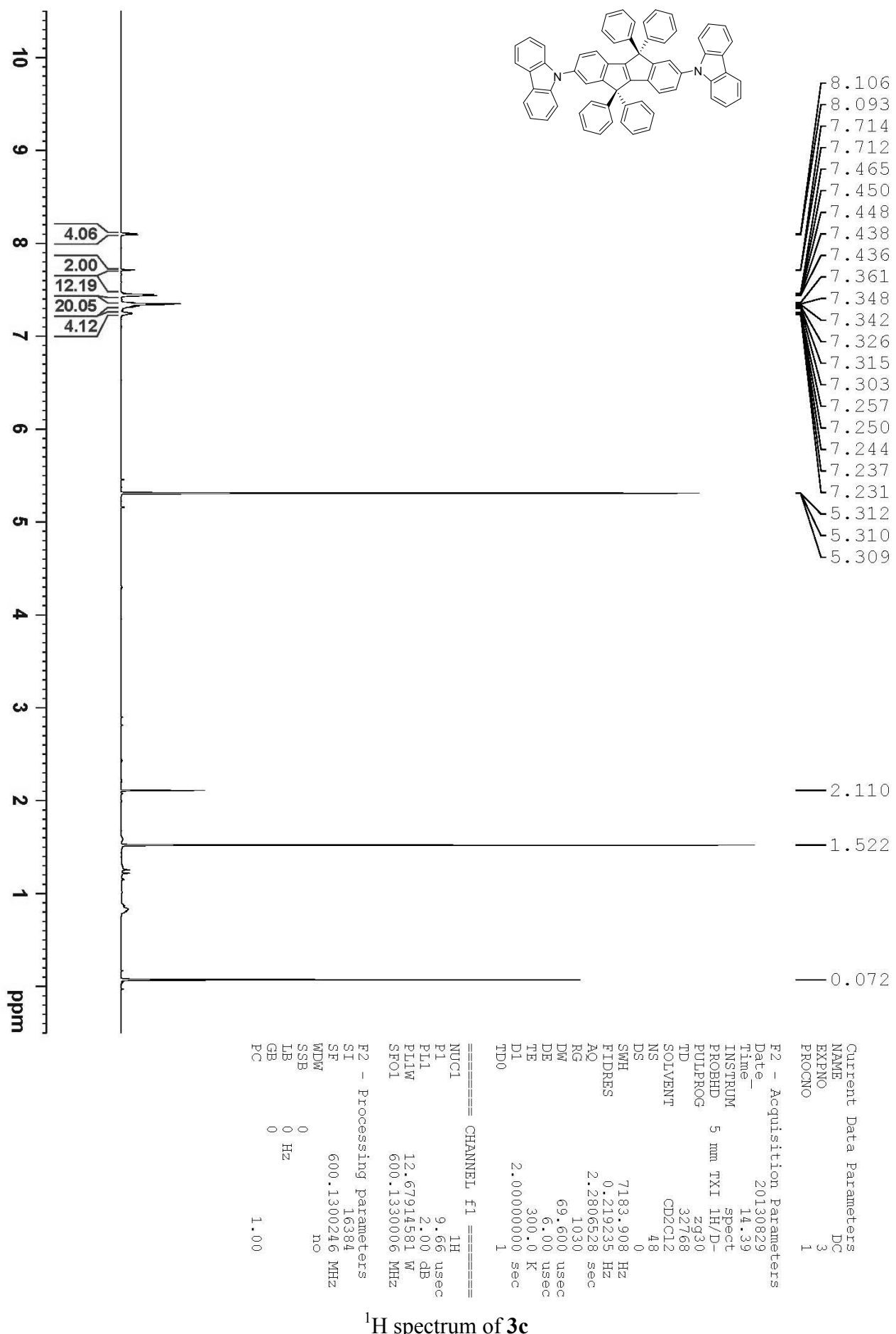
¹H spectrum of 3a



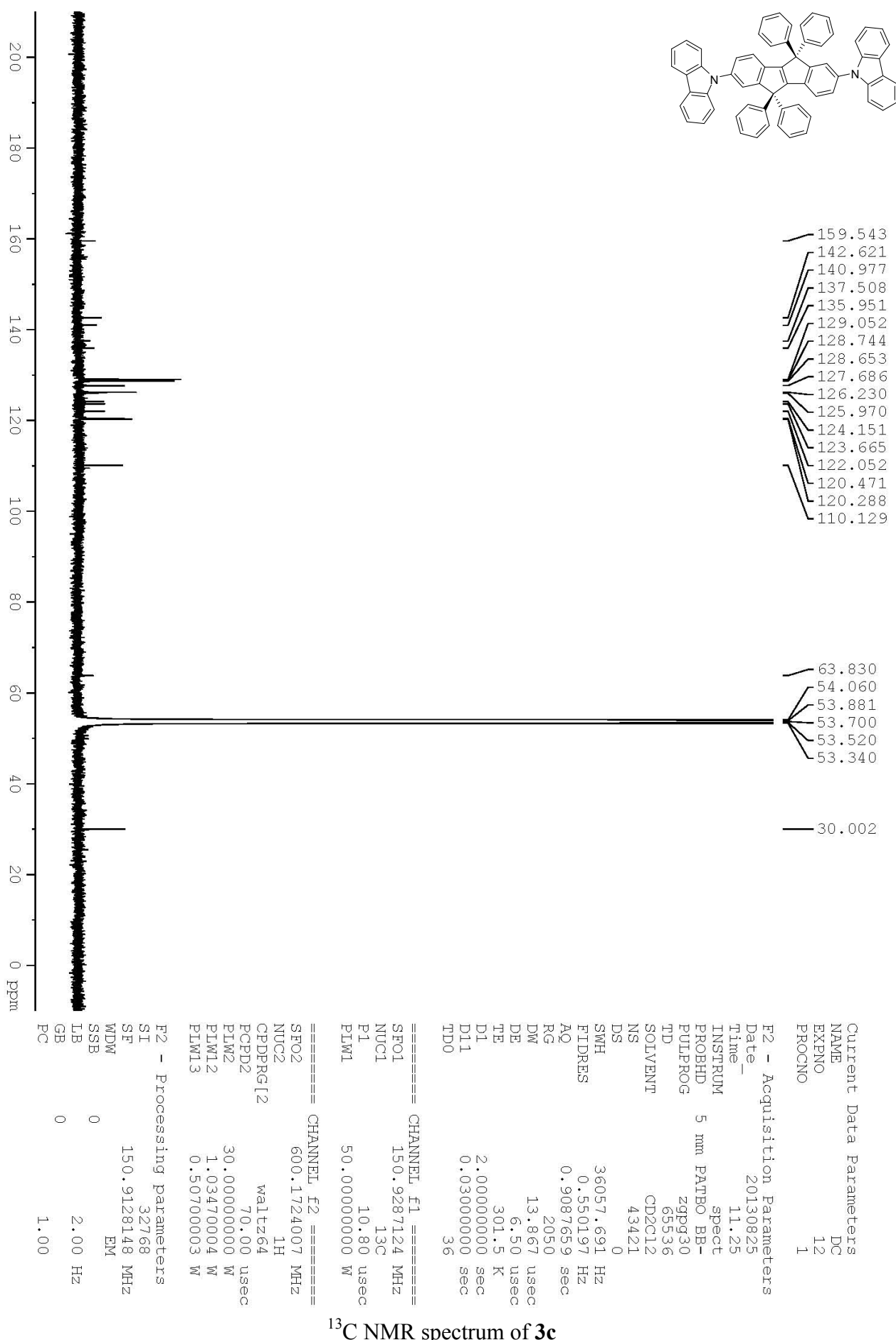


¹H spectrum of 3b





¹H spectrum of **3c**



DFT Calculation data⁵

3a

Excited State 1:	Singlet-A	2.8255 eV	438.80 nm	f=0.9099	<S**2>=0.000
222 -> 223	0.70160				
Excited State 2:	Singlet-A	3.3597 eV	369.04 nm	f=0.0002	<S**2>=0.000
221 -> 223	0.70138				
Excited State 3:	Singlet-A	3.5182 eV	352.41 nm	f=0.0039	<S**2>=0.000
221 -> 225	-0.13505				
222 -> 224	0.68181				
Excited State 4:	Singlet-A	3.5692 eV	347.37 nm	f=0.0445	<S**2>=0.000
221 -> 224	-0.15328				
222 -> 225	0.67033				
Excited State 5:	Singlet-A	3.8174 eV	324.79 nm	f=0.1069	<S**2>=0.000
221 -> 227	-0.14040				
222 -> 226	0.63792				
222 -> 227	0.10227				
222 -> 228	-0.15403				
222 -> 229	0.14966				
Excited State 6:	Singlet-A	3.8200 eV	324.56 nm	f=0.0573	<S**2>=0.000
222 -> 226	0.16705				
222 -> 228	0.66509				
Excited State 7:	Singlet-A	3.8335 eV	323.42 nm	f=0.0790	<S**2>=0.000
221 -> 226	-0.15315				
222 -> 226	-0.10005				
222 -> 227	0.65561				
222 -> 228	0.11412				
Excited State 8:	Singlet-A	3.8820 eV	319.38 nm	f=0.0400	<S**2>=0.000
221 -> 225	-0.12200				
222 -> 226	-0.13329				
222 -> 227	-0.10951				
222 -> 229	0.65285				

Excited State 9:	Singlet-A	3.9574 eV	313.30 nm	f=0.0055	<S**2>=0.000
222 -> 230	0.67726				
222 -> 231	-0.14466				
Excited State 10:	Singlet-A	3.9722 eV	312.13 nm	f=0.0121	<S**2>=0.000
221 -> 225	-0.10717				
222 -> 230	0.16519				
222 -> 231	0.62074				
222 -> 232	0.20662				

3b

Excited State 1:	Singlet-A	2.7772 eV	446.44 nm	f=0.9585	<S**2>=0.000
238 -> 239	0.70167				
Excited State 2:	Singlet-A	3.2969 eV	376.07 nm	f=0.0003	<S**2>=0.000
237 -> 239	0.70166				
Excited State 3:	Singlet-A	3.4599 eV	358.34 nm	f=0.0042	<S**2>=0.000
237 -> 241	0.13802				
238 -> 240	0.68215				
Excited State 4:	Singlet-A	3.5116 eV	353.07 nm	f=0.0421	<S**2>=0.000
237 -> 240	0.15829				
238 -> 241	0.67022				
Excited State 5:	Singlet-A	3.7462 eV	330.96 nm	f=0.0528	<S**2>=0.000
238 -> 242	0.18779				
238 -> 243	0.65232				
238 -> 244	0.12893				
Excited State 6:	Singlet-A	3.7711 eV	328.77 nm	f=0.0844	<S**2>=0.000
238 -> 242	0.57159				
238 -> 243	-0.19373				
238 -> 244	0.15720				
238 -> 245	-0.27159				
Excited State 7:	Singlet-A	3.8006 eV	326.22 nm	f=0.0885	<S**2>=0.000
237 -> 242	-0.14218				
238 -> 242	-0.27382				
238 -> 244	0.57583				
238 -> 245	-0.19791				

Excited State 8:	Singlet-A	3.8268 eV	323.99 nm	f=0.1215	<S**2>=0.000
237 -> 244	-0.14475				
238 -> 242	0.15918				
238 -> 244	0.28174				
238 -> 245	0.58470				
Excited State 9:	Singlet-A	3.8876 eV	318.92 nm	f=0.0068	<S**2>=0.000
238 -> 246	0.65547				
238 -> 247	-0.22636				
Excited State 10:	Singlet-A	3.8990 eV	317.99 nm	f=0.0262	<S**2>=0.000
238 -> 246	0.23060				
238 -> 247	0.61620				
238 -> 248	0.17562				

3c

Excited State 1:	Singlet-A	3.0249 eV	409.88 nm	f=0.6741	<S**2>=0.000
220 -> 221	0.70200				
Excited State 2:	Singlet-A	3.3077 eV	374.84 nm	f=0.0000	<S**2>=0.000
219 -> 221	0.70276				
Excited State 3:	Singlet-A	3.6837 eV	336.58 nm	f=0.0001	<S**2>=0.000
217 -> 221	0.15110				
218 -> 221	0.68751				
Excited State 4:	Singlet-A	3.6838 eV	336.56 nm	f=0.0000	<S**2>=0.000
217 -> 221	0.68767				
218 -> 221	-0.15118				
Excited State 5:	Singlet-A	3.7766 eV	328.30 nm	f=0.0903	<S**2>=0.000
216 -> 221	0.68980				
Excited State 6:	Singlet-A	3.8805 eV	319.51 nm	f=0.0000	<S**2>=0.000
219 -> 225	-0.14402				
220 -> 224	0.66232				
Excited State 7:	Singlet-A	3.9191 eV	316.36 nm	f=0.0627	<S**2>=0.000
219 -> 222	0.29998				
220 -> 223	0.59870				
220 -> 225	0.13859				

Excited State 8:	Singlet-A	3.9203 eV	316.26 nm	f=0.0000	<S**2>=0.000
219 -> 223	0.30809				
220 -> 222	0.61561				
Excited State 9:	Singlet-A	3.9447 eV	314.30 nm	f=0.0168	<S**2>=0.000
214 -> 221	0.13274				
219 -> 224	-0.19669				
220 -> 223	-0.12619				
220 -> 225	0.60710				
220 -> 226	0.11053				
Excited State 10:	Singlet-A	4.2099 eV	294.51 nm	f=0.0551	<S**2>=0.000
219 -> 224	-0.13153				
220 -> 225	-0.19102				
220 -> 226	0.64666				

References

1. G. II. Jones, W. R. Jackson, C.-Y. Choi and W. R. Bergmark, *J. Phys. Chem.* 1985, **89**, 294.
2. A. Caruso, M. A. Siegler and J. D. Tovar, *Angew. Chem. Int. Ed.* 2010, **122**, 4309.
3. X. Zhu, H. Tsuji, K. Nakabayashi, S. Ohkoshi and E. Nakamura, *J. Am. Chem. Soc.* 2011, **133**, 16342.
4. J. F. Hartwig, *Acc. Chem. Res.* 1998, **31**, 852.
5. M. J. Frisch, G. W. Trucks, H. B. Schlegel, G. E. Scuseria, M. A. Robb, J. R. Cheeseman, G. Scalmani, V. Barone, B. Mennucci, G. A. Petersson, H. Nakatsuji, M. Caricato, X. Li, H. P. Hratchian, A. F. Izmaylov, J. Bloino, G. Zheng, J. L. Sonnenberg, M. Hada, M. Ehara, K. Toyota, R. Fukuda, J. Hasegawa, M. Ishida, T. Nakajima, Y. Honda, O. Kitao, H. Nakai, T. Vreven, J. A. Jr. Montgomery, J. E. Peralta, F. Ogliaro, M. Bearpark, J. J. Heyd, E. Brothers, K. N. Kudin, V. N. Staroverov, R. Kobayashi, J. Normand, K. Raghavachari, A. Rendell, J. C. Burant, S. S. Iyengar, J. Tomasi, M. Cossi, N. Rega, N. J. Millam, M. Klene, J. E. Knox, J. B. Cross, V. Bakken, C. Adamo, J. Jaramillo, R. Gomperts, R. E. Stratmann, O. Yazyev, A. J. Austin, R. Cammi, C. Pomelli, J. W. Ochterski, R. L. Martin, K. Morokuma, V. G. Zakrzewski, G. A. Voth, P. Salvador, J. J. Dannenberg, S. Dapprich, A. D. Daniels, Ö. Farkas, J. B. Foresman, J. V. Ortiz, J. Cioslowski and D. J. Fox, *Gaussian 09, Revision D.01*, Gaussian, Inc.: 2009.